Comparative performance of upflow anaerobic sludge blanket reactor and anaerobic membrane bioreactor treating phenolic wastewater

Overcoming high salinity

Muñoz Sierra, Julian D.; Oosterkamp, Margreet J.; Wang, Wei; Spanjers, Henri; van Lier, Jules B.

DOI
10.1016/j.cej.2019.02.097

Publication date
2019

Document Version
Final published version

Published in
Chemical Engineering Journal

Citation (APA)
Muñoz Sierra, J. D., Oosterkamp, M. J., Wang, W., Spanjers, H., & van Lier, J. B. (2019). Comparative performance of upflow anaerobic sludge blanket reactor and anaerobic membrane bioreactor treating phenolic wastewater: Overcoming high salinity. *Chemical Engineering Journal*, *366*, 480-490. https://doi.org/10.1016/j.cej.2019.02.097

Chemical Engineering Journal 366 (2019) 480–490

Contents lists available at ScienceDirect

Chemical Engineering Journal

journal homepage: www.elsevier.com/locate/cej

Comparative performance of upflow anaerobic sludge blanket reactor and anaerobic membrane bioreactor treating phenolic wastewater: Overcoming high salinity

Julian D. Muñoz Sierra[a,*], Margreet J. Oosterkamp[a], Wei Wang[a,b], Henri Spanjers[a], Jules B. van Lier[a]

[a] Department of Water Management, Section Sanitary Engineering, Delft University of Technology, Stevinweg 1, 2628 CN Delft, The Netherlands
[b] Department of Municipal Engineering, School of Civil and Hydraulic Engineering, Hefei University of Technology, Hefei 230009, China

HIGHLIGHTS

- AnMBR exhibited higher stability than the UASB to overcome high salinity.
- Long-term calcium wash-out led the UASB to failure at 26 $gNa^{+}L^{-1}$.
- UASB showed lower species evenness and methanogenic activity than the AnMBR.
- AnMBR exhibited a phenol removal of 96% at 26 $gNa^{+}L^{-1}$.
- High salinity significantly decreased biomass particle size in both reactors.

GRAPHICAL ABSTRACT

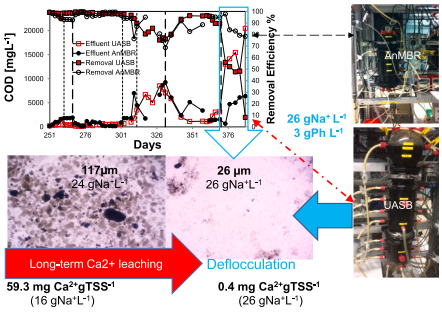

ARTICLE INFO

Keywords:
AnMBR
UASB
Salinity
Phenol
Microbial dynamics
Deflocculation

ABSTRACT

Anaerobic membrane bioreactors (AnMBRs) offer an attractive option for treating industrial wastewaters under extreme conditions that might hamper granulation, biomass retention and reduce biological activity. This study assesses the long-term performance of an upflow anaerobic sludge blanket reactor (UASB) and an AnMBR treating highly saline phenolic wastewater. Analysis of bioreactor conversion, biomass characteristics and microbial community dynamics under increasing sodium and phenol concentrations is presented. The results demonstrated that compared to the UASB, the AnMBR process exhibited higher stability, likely due to its enhanced biomass retention. The AnMBR retained specialized microorganisms under increasing influent concentrations of phenol up to 5 $gPh{\cdot}L^{-1}$ and salinity up to 26 $gNa^{+}{\cdot}L^{-1}$. In contrast, when the UASB reached this high influent phenol and high sodium concentration, deflocculation of biomass, apparently due to calcium leaching, was observed leading to a severe conversion capacity loss. Microbial community dynamics showed higher species evenness in the AnMBR compared to the UASB, leading to a higher methanogenic ability to respond to disturbances such as high phenol and sodium concentration increases. These findings highlighted the promising features of AnMBR technology, in widening the application potentials of high-rate anaerobic wastewater treatment and overcoming specific challenges in the treatment of chemical wastewater streams under extreme environmental conditions such as high salinity.

* Corresponding author at: KWR Watercycle Research Institute, Groningenhaven 7, 3430 BB Nieuwegein, The Netherlands.
E-mail addresses: J.D.MunozSierra@tudelft.nl, julian.munoz@kwrwater.nl (J.D. Muñoz Sierra).

https://doi.org/10.1016/j.cej.2019.02.097
Received 2 December 2018; Received in revised form 7 February 2019; Accepted 13 February 2019
Available online 14 February 2019

1. Introduction

The current challenges of industrial wastewater treatment include degradation of a large variety of contaminants such as phenols and other aromatic compounds under high salt concentrations typical of olive oil mills, oil refineries, textile, coal gasification, and petrochemical industries [1,2]. Research on both aerobic [3,4] and anaerobic [5,6] treatment technologies are dealing with these types of wastewaters with emphasis on the limitations associated with high salinity or phenol toxicity. From the two alternatives, high-rate anaerobic treatment receives major interest owing to its positive energy footprint and other advantages associated with it. Sludge bed based technologies such as the upflow anaerobic sludge blanket (UASB) reactor, are thus far considered the most cost-effective at industrial scale for chemical wastewaters [7]. In order to apply high organic loading rates and improved hydraulic mixing e.g. by effluent recycling, a proper sludge granulation process is of eminent importance in sludge bed reactors treating these wastewaters. Moreover, as a result of mass transfer limitation phenomena, the granule structure will protect functional microorganisms at the core of the granule from inhibitory and toxic pollutants [8]. Sludge granulation is difficult to accomplish at high salinity because salinity reduces microbial growth and induces the disintegration of flocs and granules leading to a prominent biomass wash-out and induces the disintegration of flocs and granules leading to a prominent biomass wash-out [9,10]. However, thanks to the presence of an absolute barrier, the achievable treatment efficiencies in anaerobic membrane bioreactors (AnMBRs) are independent of sludge settling properties or sludge granulation. The solids retention time (SRT) in AnMBRs is fully governed by the sludge discharge, giving ample possibilities for enrichment with specialized microbial consortia [11]. AnMBRs are generally equipped with Ultrafiltration (UF) membranes, which additionally offer high-quality effluents free of solids, facilitating downstream water recovery [12]. Therefore, regardless their increased costs, AnMBRs may offer an attractive option for treating industrial wastewaters under extreme environmental conditions that hamper granulation, effective biomass retention and reduced biological activity [7], such as high salinity and the presence of toxic compounds [13].

To the best of our knowledge, only two studies have attempted to treat highly saline phenolic wastewater using high-rate anaerobic technologies [14,15]. Wang et al. [14] used UASB reactors treating wastewater containing 10 and 20 $gNa^{+}{\cdot}L^{-1}$ in a range of total phenol concentrations (TPh) between 0.1 and 2.0 $gTPh{\cdot}L^{-1}$. At 10 $gNa^{+}{\cdot}L^{-1}$ and 1.0 $gTPh{\cdot}L^{-1}$ the phenol conversion and specific methanogenic activity (SMA) decreased about 57% and 37%, respectively, compared to a non-saline UASB control reactor, whereas either at 20 $gNa^{+}{\cdot}L^{-1}$ or 2.0 $gTPh{\cdot}L^{-1}$ the SMA was reduced by about 75% and 79%, respectively, and a severe inhibition of phenol degradation was observed. On the other hand, Muñoz Sierra et al. [15] evaluated the impact of long-term salinity increase to 20 $gNa^{+}{\cdot}L^{-1}$ on the bioconversion of phenol in an AnMBR treating an influent with concentrations up to 0.5 $gPh{\cdot}L^{-1}$. The treatment performance of the researched AnMBR remained stable irrespective the salinity changes, resulting in an endured microbial community and 56% higher phenol conversion rates when salinity increased from 16 $gNa^{+}{\cdot}L^{-1}$ to 20 $gNa^{+}{\cdot}L^{-1}$.

In order to determine which type of reactor system, UASB or AnMBR, would be more suitable for treating chemical wastewaters under extreme conditions, a comparative study was performed in which both reactor systems were exposed to the same extreme sodium and phenol loadings conditions. It is hypothesized that by increasing both the sodium and phenol influent concentrations the capacity limits of either system will be reached. A UASB reactor is fully dependent on active well-settling or granular biomass, whereas the suspended biomass in the AnMBR system might become more susceptible for increasing phenol concentrations in the bulk of the reactor broth. However, since all biomass is retained in an AnMBR, the latter could be overcome by in-situ bioaugmentation of the proper phenol degrading consortia. A phenomenon that is likely less apparent in a UASB where the biomass is prone to wash-out. In the present comparative study, the treatment performance of both a UASB and a completely mixed AnMBR under increasing sodium and phenol influent concentrations is assessed. In addition, a comprehensive analysis of the properties of the two types of biomass coming from both reactors, i.e, granular and suspended, was performed, whereas the microbial community dynamics and diversity was analyzed.

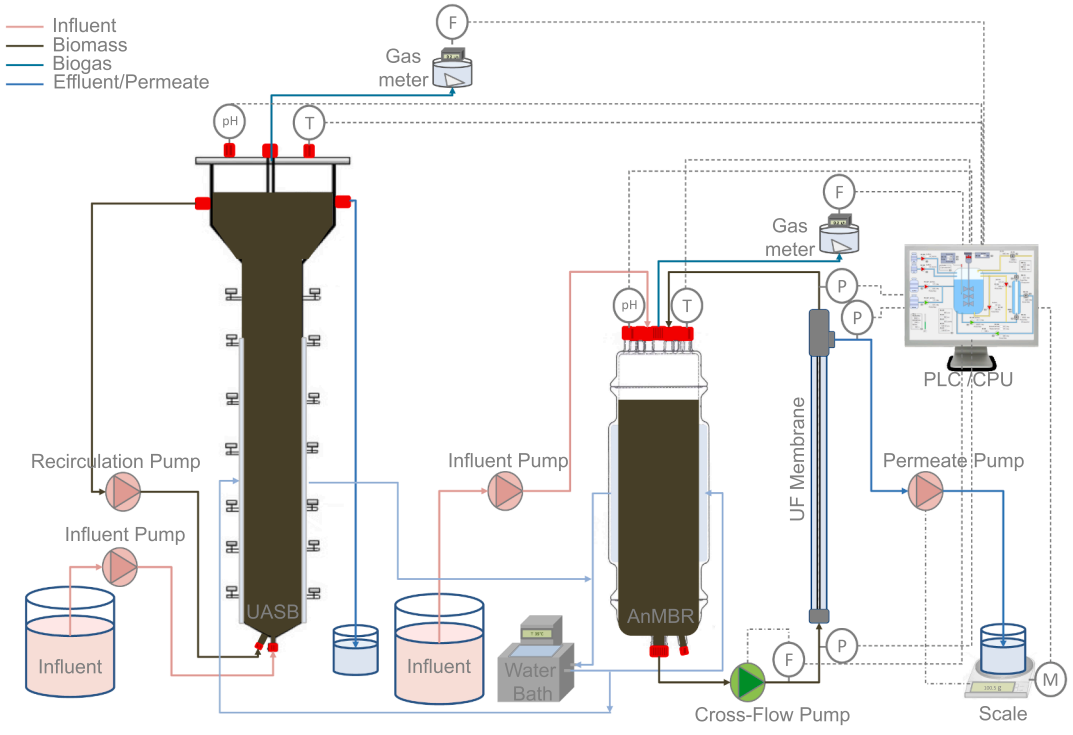

Fig. 1. Schematic illustration of UASB and AnMBR setup.

2. Material and methods

2.1. Reactors configuration and operation

The experiments were performed using laboratory scale AnMBR and UASB reactors, both with an effective volume of 7 L. A schematic diagram of the reactor configurations is depicted in Fig. 1. The completely mixed AnMBR was equipped with a side-stream ultrafiltration (UF) membrane module. A tubular PVDF membrane (Pentair X-Flow, The Netherlands) with 5.2 mm inner diameter and 0.64 m length was used. Transmembrane pressure (TMP) was monitored using three pressure sensors (AE Sensors ATM, The Netherlands). The AnMBR was equipped with feed, recycle and effluent pumps (Watson-Marlow 120U/DV, 220Du) and the UASB with feed and effluent recirculation pump (Watson-Marlow 120U/DV). The AnMBR was completely mixed due to a turnover of 170 with a cross-flow velocity of 0.65 $m{\cdot}s^{-1}$. A flux of about 4 $Lm^{-2}h^{-1}$ was maintained. The UASB reactor was operated with an up-flow velocity of 0.6 $m{\cdot}h^{-1}$. The biogas was collected by means of a three-phase separator installed at the top of the UASB reactor. The reactors were equipped with pH and temperature sensors (Endress & Hauser, Memosens), and biogas flow-rate meters (Ritter, Milligas Counter MGC-1 PMMA, Germany). The temperature of the jacketed reactors was controlled by thermostatic water baths (Tamson Instruments, The Netherlands). The setups were controlled by a computer running LabView software (version 15.0.1f1, National Instruments, USA).

The sodium concentration in the reactors was increased from 12 $gNa^{+}{\cdot}L^{-1}$ to 16 $gNa^{+}{\cdot}L^{-1}$ for a period of 155 days before the comparison study started, with a further increase to 26 $gNa^{+}{\cdot}L^{-1}$ until day 388 in four phases. Influent phenol concentrations from 0.2 $gPh{\cdot}L^{-1}$ up to 5 $gPh{\cdot}L^{-1}$ were applied. During the operation of the reactors, the biomass concentration in the UASB decreased mainly due to wash-out from 19.3 $gVSS{\cdot}L^{-1}$ at 8 $gNa^{+}{\cdot}L^{-1}$ to a stable concentration of 5.9 $gVSS{\cdot}L^{-1}$ at 16 $gNa^{+}{\cdot}L^{-1}$ on day 155 (initial day of this study). In the case of the AnMBR, at day 155 and the same salinity, the biomass concentration was about 15.2 $gVSS{\cdot}L^{-1}$. The temperature and pH were maintained at 35 ± 0.8 °C and 8.0 ± 2.0 in both reactors. HRT and SRT were kept average about 7 d and 40 ± 2 d in both reactors. The main operational conditions along the experiment are summarized in Table 1.

2.2. Inoculum source and synthetic wastewater composition

The two reactors were inoculated with mesophilic anaerobic biomass obtained from a full-scale UASB reactor (Shell, Moerdijk, The Netherlands). The synthetic wastewater consisted of sodium acetate ($C_2H_3NaO_2$), and phenol (C_6H_6O) with varying concentrations according to the applied phenol loading rates (PhLR). The amount of sodium chloride (NaCl), solution of K_2HPO_4 (34.85 gL^{-1}) and solution of NaH_2PO_4 (24 g L^{-1}) varied according to the sodium concentration applied in the reactor in each phase, maintaining a K^{+}:Na^{+} ratio of 0.05 [15]. Yeast extract (2.0 g L^{-1}), macronutrients (9 mL L^{-1}), and micronutrients (4.5 mL L^{-1}) solutions were added (Table 2). The chemical reagents were of analytical grade.

Table 2
Synthetic wastewater composition.

		Phase I	Phase II	Phase III	Phase IV
C_6H_6O [$gPh{\cdot}L^{-1}$]		0.5–1.5	1.5–5.0	3.0	3.0
Total Na^{+} [gNa^{+} L^{-1}]		16	18	24	26
Macronutrient solution [g L^{-1}]		Micronutrient solution [g L^{-1}]			
NH_4Cl	170	$FeCl_3{\cdot}6H_2O$	2	$(NH_4)_6Mo_7O_2{\cdot}4H_2O$	0.09
$CaCl_2{\cdot}2H_2O$	8	$CoCl_2{\cdot}6H_2O$	2	Na_2SeO_3	0.1
$MgSO_4{\cdot}7H_2O$	9	$MnCl_2{\cdot}4H_2O$	0.5	$NiCl_2{\cdot}6H_2O$	0.05
		$CuCl_2{\cdot}2H_2O$	0.03	EDTA	1
		$ZnCl_2$	0.05	Na_2WO_4	0.08
		H_3BO_3	0.05		

2.3. Permeate characterization

2.3.1. Phenol and COD analysis

Phenol concentrations were measured using high-pressure liquid chromatography HPLC LC-20AT (Shimadzu, Japan) equipped with a 4.6 mm reversed phase C18 column (Phenomenex, The Netherlands) and a UV detector at a wavelength of 280 nm. The mobile phase used was 25% (v/v) acetonitrile at a flow rate of 0.95 mL min^{-1}. The column oven was set at 30 °C. Quick phenol measurements were done by Merck – Spectroquant® Phenol cell kits using a spectrophotometer NOVA60 (Merck, Germany). Hach Lange kits were used to measure chemical oxygen demand (COD). Corresponding dilutions were made to avoid measurements interference by high salinity. The COD was measured using a VIS - spectrophotometer (DR3900, Hach Lange, Germany).

2.3.2. Calcium and sodium profiles from permeate and biomass matrix

Calcium and sodium effluent concentrations were measured by Ion Chromatography (IC 883 – Basic IC Plus, Metrohm, Switzerland) with a Metrosep C4 – 150/4.0 column and Metrosep RP2 Guard/3.5 guard column and as eluent 3 mM HNO_3 (at 0.9 mL/min). Dilutions were applied to samples and were prepared in triplicates. Calibration curves were made using AAS standard solutions (Sigma-Aldrich) in the range between 0.1 and 50 ppm. The final concentrations were calculated by using the MagIC Net software.

Biomass samples of 1 gTSS were destructed with Agua regia (mixture of 2.5 mL 65% HNO_3 and 7.5 mL 37% HCl) in a microwave reaction system (MultiwavePRO, Anton Paar GmbH, Austria) following the procedure described by Ismail et al. [16]. After the digestion, liquid samples were analyzed by Inductively Coupled Plasma Optical Emission Spectroscopy (Optima 5300DV, Perkin Elmer Instruments, USA) to determine calcium concentrations.

2.4. Biomass characteristics

2.4.1. Soluble microbial products (SMP) and extracellular polymeric substances (EPS)

SMP and EPS were characterized based on proteins and polysaccharides. EPS extraction was carried out by cation exchange resin method. The functional groups of EPS extracted at different phases were identified with a Fourier Transform Infrared (FT-IR) Spectrometer (Spectrum 100 Series Perkin–Elmer, UK) as explained by Muñoz Sierra

Table 1
Reactors operational conditions.

Day	Sodium[$gNa^{+}L^{-1}$]	OLR[$gCOD{\cdot}L^{-1}{\cdot}d^{-1}$]	PhLR[$gPh{\cdot}L^{-1}{\cdot}d^{-1}$]	$Biomass_{UASB}$[$gVSS{\cdot}L^{-1}$]	$Biomass_{AnMBR}$[$gVSS{\cdot}L^{-1}$]	Phase (Period)
155	16	5.50	0.11	5.9	15.2	I (Day 155–261)
187	16	5.50	0.11	6.1	11.2	I (Day 155–261)
280	18	5.70	0.33	8.6	12.7	II (Day 262–332)
322	18	7.64	1.11	10.9	12.7	II (Day 262–332)
357	24	6.57	0.67	6.4	13.5	III (Day 333–371)
379	26	6.57	0.67	7.9	16.7	IV (Day 372–388)

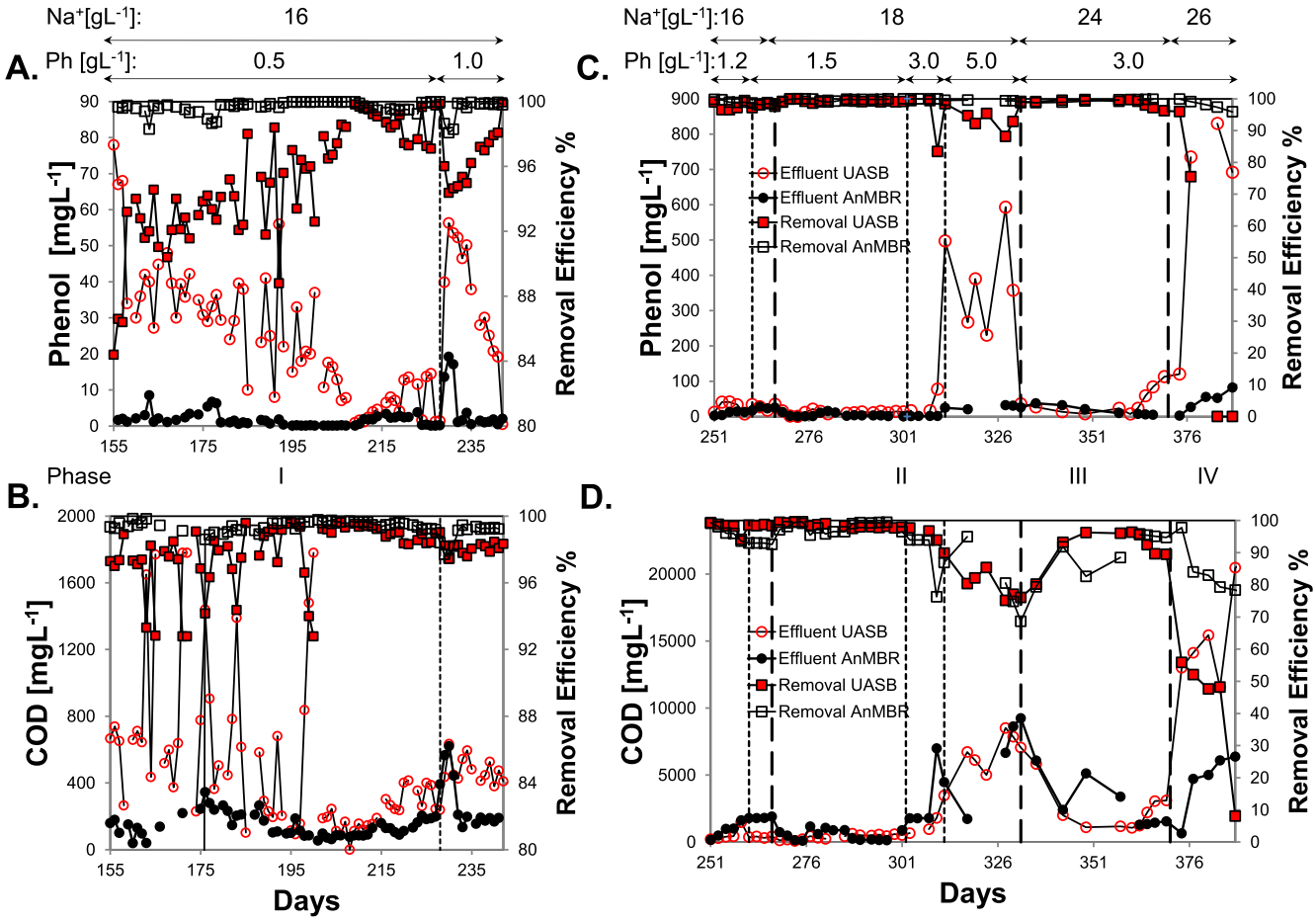

Fig. 2. Reactors performance. Effluent phenol concentration and removal efficiency A. Phase I , C. Phases II-IV. Effluent COD concentration and removal efficiency B. Phase I , D. Phases II-IV.

et al. [6]. EPS was normalized against the biomass VSS concentration in the reactor.

2.4.2. Particle size distribution (PSD)

PSD measurements were carried out by using a DIPA-2000 EyeTech™ particle analyzer (Donner Technologies, Or Akiva, Israel) with an A100 and B100 laser lens (measuring range 0.1–300 µm and 1–2000 µm, respectively) and a liquid flow cell DCM-104A (10 × 10 mm). Furthermore, deflocculation was further studied using a digital microscope (Keyence VHX-5000) with VH-Z20UR lens set and 100× magnification.

2.4.3. Specific methanogenic activity (SMA) tests

SMA tests were performed in triplicate using an automated methane potential test system (AMPTS, Bioprocess Control, Sweden). All the SMA tests were carried out at 35 °C following the method described by van Loosdrecht et al. [17].

2.5. Microbial community and statistical analysis

2.5.1. DNA extraction and sequencing

DNA extraction was performed from both reactors' biomass samples by using the DNeasy UltraClean Microbial kit (Qiagen, Hilden, Germany). Qubit3.0 DNA detection (Qubit® dsDNA HS Assay Kit, Life Technologies, U.S.) and agarose gel electrophoresis were used to check the quantity and quality of the DNA extracted. 16S rRNA gene amplicon sequencing was carried out by the MiSeq Illumina platform and using the primers 341F (5′-CCTACGGGNGGCWGCAG-3′) 785R (5′-GACTACHVGGGTATCTAATCC-3′) for bacteria/archaea in the V3-V4 region (BaseClear, Leiden, the Netherlands). The sequences were analyzed using the QIIME pipeline (version 1.9.0). Demultiplexing and quality filtering were performed with Q = 20, r = 3, and p = 0.75 parameters. Chimeric sequences were removed with the UCHIME2 (version 9.0) [18]. Sequences were clustered into operational taxonomic units (OTUs) with a 97% similarity as the cutoff, with UCLUST algorithm [19]. Singletons were removed and OTUs with an occurrence less than three times in at least one sample were excluded. Taxonomic assignation was performed using the Silva database (SILVA-128) with UCLUST. For beta diversity, separate non-metric distance scaling (NMDS) analysis of the microbial community was made based on the unweighted Unifrac distance measure. Alpha diversity was analyzed following the guidelines of Hill [20]. Beta diversity plots were generated with the phyloseq and ggplot2 packages in the R environment. The sequences reported in this paper have been deposited in the NCBI SRA under the accession number SRP149410.

2.5.2. Fluorescent in situ hybridization (FISH)

Biomass samples taken from the AnMBR and UASB reactors were treated as cell suspensions and fixed on paraformaldehyde according to a procedure described previously and followed by DAPI staining [21]. Archaea were Cy3-stained using the Arc 915 Cy3 FISH oligonucleotide probe. Hybridized biomass samples were examined with a Zeiss Axioplan-2 epifluorescence microscope and Axiovision (release 4.8.2) software (Zeiss, Germany).

2.5.3. Statistical analysis

Statistical differences between the two reactors and among the reactor samples under different conditions were evaluated using ANOSIM

and ADONIS analysis in the QIIME pipeline. Two comparing data sets were considered statistically different when a *p-value* ≤ 0.05 was determined. A *t*-test was done to determine statistical differences between the Alpha diversity measures.

3. Results and discussion

3.1. UASB and AnMBR reactors performance and conversion rates

UASB and AnMBR reactors treating phenolic wastewater were subjected to increasing sodium concentrations. Phenol removal efficiencies fluctuated between 84.4% and 99.8% in the UASB and a more stable removal of 98.1%–99.9% was observed in the AnMBR at 16 $gNa^+·L^{-1}$ and influent phenol concentration of 0.5 $gPh·L^{-1}$ (Phase I, Fig. 2A). The corresponding phenol loading rate (PhLR) was 0.11 $gPh·L^{-1}·d^{-1}$ (Table 1). Thereby, the AnMBR showed a lower total COD effluent concentration than the UASB reactor when operated at 16 $gNa^+·L$ (Fig. 2B) and an OLR of 5.50 $gCOD·L^{-1}·d^{-1}$. However, the UASB reactor showed gradual improvement within days 155 and 228 showing lower effluent phenol concentrations, dropping from 68 $mgPh·L^{-1}$ to 1.2 $mgPh·L^{-1}$ respectively, indicating biomass adaptation to this sodium concentration (Fig. 2A).

Both AnMBR and UASB reactors coped well with an increase in influent phenol concentrations from 0.5 to 1.0 and 1.2 $gPh·L^{-1}$ (Phase II, Fig. 2C). The AnMBR showed higher stability most likely due to its higher biomass concentration at a PhLR of 0.27 $gPh·L^{-1}·d^{-1}$ on day 260. At 18 $gNa^+·L^{-1}$ (Phase II) and 1.5 $gPh·L^{-1}$, both reactors exhibited a very stable phenol degradation performance (Fig. 2C), which is attributed to the long-term adaptation process of the microbial community. The latter suggested that the reactors could manage a higher phenol loading rate and thereby their phenol bioconversion could be maximized. The UASB phenol degradation rate was about 38.6 $mgPh·gVSS^{-1}·d^{-1}$ and for the AnMBR this was about 26.1 $mgPh·gVSS^{-1}·d^{-1}$ under the above mentioned conditions. The AnMBR effluent reached lower phenol concentrations of about 0.88 $mgPh·L^{-1}$ compared to the UASB (13.5 $mgPh·L^{-1}$). At phenol influent concentration of 3.0 $gPh·L^{-1}$ and a PhLR of 0.67 $gPh\ L^{-1}·d^{-1}$ the removal efficiency of the UASB reactor decreased to 83.4% with a phenol conversion rate of 76 $mgPh·gVSS^{-1}·d^{-1}$ (Phase II, Fig. 2C). This is in agreement with Wang et al. [14] who found that a UASB reactor performs well under an influent concentration of total phenols lower than 1.0 $g.L^{-1}$ and 10 gNa^+L^{-1}, but shows severe removal limitations (about 40% efficiency) when 2.0 $gPh·L^{-1}$ and 20 $gNa^+·L^{-1}$ are applied. The AnMBR phenol degradation rate was lower, i.e. 53 $mgPh·gVSS^{-1}·d^{-1}$ but with a 16% higher removal efficiency than the UASB. When the influent phenol concentration was increased to 5 $gPh·L^{-1}$, both reactors had a similar reduction in COD removal efficiency to about 70% (Phase II, Fig. 2D) at an OLR of 7.64 $gCOD·L^{-1}·d^{-1}$. However, phenol concentration increased to 600 $mgPh\ L^{-1}$ in the UASB effluent, whereas the AnMBR kept a low phenol concentration of 25 $mgPh·L^{-1}$ (Fig. 2C). The phenol conversion rates were 87.4 $mgPh·gVSS^{-1}·d^{-1}$ and 97.7 $mgPh·gVSS^{-1}·d^{-1}$ for the AnMBR and the UASB reactor, respectively (Table 3). The observed phenol degradation rates were higher than reported in previous studies using AnMBR or UASB under high phenol and high sodium concentrations [14,15].

Under an increasing salinity from 18 $gNa^+·L^{-1}$ to 24 $gNa^+·L^{-1}$ (Phase III) and a reduced influent phenol concentration of 3.0 $gPh·L^{-1}$ (PhLR of 0.67 $gPh·L^{-1}·d^{-1}$) the reactors recovered their COD removal efficiencies to values exceeding 90% (Phase III, Fig. 2D). Under this level of salinity, De Vrieze et al.[22] reported a COD removal of only 4.9 ± 0.8% at 20 $gNa^+·L^{-1}$ and severe inhibition of methanogenesis in CSTR reactors. The abrupt salinity increase initially did not appear to have a negative effect on the phenol conversion rate in the UASB reactor, contrasting the results obtained in the AnMBR in which a reduction from 87.4 to 49.4 $mgPh·gVSS^{-1}·d^{-1}$ was found. However, the effluent concentration of the UASB increased gradually to 113 $mgPh·L^{-1}$ on day 370. Conversely, the COD removal efficiency of the UASB started to decrease at the end of phase III. These observations are in agreement with Muñoz Sierra et al. [15] who observed that a one-step salinity increase of 4 $gNa^+·L^{-1}$ already reduces the quality and biological stability of the biomass.

In Phase IV, the UASB phenol effluent concentration increased to about 830 $mgPh·L^{-1}$, and the phenol conversion rate decreased remarkably from 103.2 to 32.90 $mgPh·gVSS^{-1}·d^{-1}$ at day 379 (Phase IV, Fig. 2C). A very poor bioreactor performance was observed compared to the AnMBR at a sodium concentration of 26 $gNa^+·L^{-1}$. A COD removal efficiency of 47% was observed before the biomass started to wash-out. Aslan and Şekerdağ [23] reported a significant decrease in COD removal efficiency at a sodium concentration of about 20 $gNa^+·L^{-1}$ in a UASB treating highly saline glucose containing wastewater. A severe deflocculation phenomenon was observed in the UASB, as further explained, leading to reactor failure. Jeison and van Lier [10] observed that high salinity conditions (20 $gNa^+·L^{-1}$) in a UASB results in sodium inhibition. In contrast, this level of salinity made the AnMBR performance unstable but it continued performing with phenol and COD removal efficiencies of 96% and 80%, respectively, demonstrating that a membrane enhanced biomass retention was needed to overcome biomass losses resulting from high sodium concentration.

The specific methanogenic activities (SMAs) of the biomasses in both reactors are shown in Table 3. SMAs were similar in phases I and II before the phenol loading rate was increased to 1.11 $gPh·L^{-1}·d^{-1}$ On day 322, at the end of phase II, the SMA of the UASB biomass decreased to 0.39 ± 0.08 $gCOD\text{-}CH_4·gVSS^{-1}·d^{-1}$ compared to 0.64 ± 0.01 $gCOD\text{-}CH_4·gVSS^{-1}·d^{-1}$ of the AnMBR. Chapleur et al. [24] observed that the anaerobic cellulose digestion was progressively affected as phenol concentration increased and that methanogenesis was the most sensitive step with SMA half-inhibition concentration of 1.40 $gPh·L^{-1}$. Furthermore, in this study the increase in influent sodium concentrations by a step of 6 $gNa^+·L^{-1}$ in phase III affected the SMA in the AnMBR resulting in values lower than half of the SMA observed at 18 $gNa^+·L^{-1}$, suggesting that the half-inhibition sodium concentration (IC_{50}) was already reached as described by Muñoz Sierra et al. [13]. In

Table 3
SMA, phenol conversion and COD removal rates at different sodium concentrations.

Phase	Sodium[$gNa^+·L^{-1}$]	Day	SMA [$gCOD\text{-}CH_4·gVSS^{-1}·d^{-1}$]		Phenol conversion rate [$mgPh·gVSS^{-1}·d^{-1}$]		COD removal rate [$gCOD·gVSS^{-1}·d^{-1}$]	
			UASB	AnMBR	UASB	AnMBR*	UASB	AnMBR*
I	16	155	0.50 ± 0.05	0.42 ± 0.04	15.7	7.4	1.22	0.50
	16	187	0.76 ± 0.06	0.87 ± 0.01	17.6	9.9	0.89	0.49
II	18	280	0.44 ± 0.10	0.65 ± 0.02	38.6	26.1	0.65	0.44
	18	322	0.39 ± 0.08	0.64 ± 0.01	97.7	87.4	0.60	0.49
III	24	357	0.29 ± N.D**	0.31 ± 0.04	103.2	49.4	0.98	0.43
IV	26	379	0.16 ± N.D**	0.25 ± 0.05	32.9	40.1	0.40	0.39

*AnMBR biomass concentration was higher than the UASB, indicating that the reactor was under loaded. **Replicates were not available for these samples.

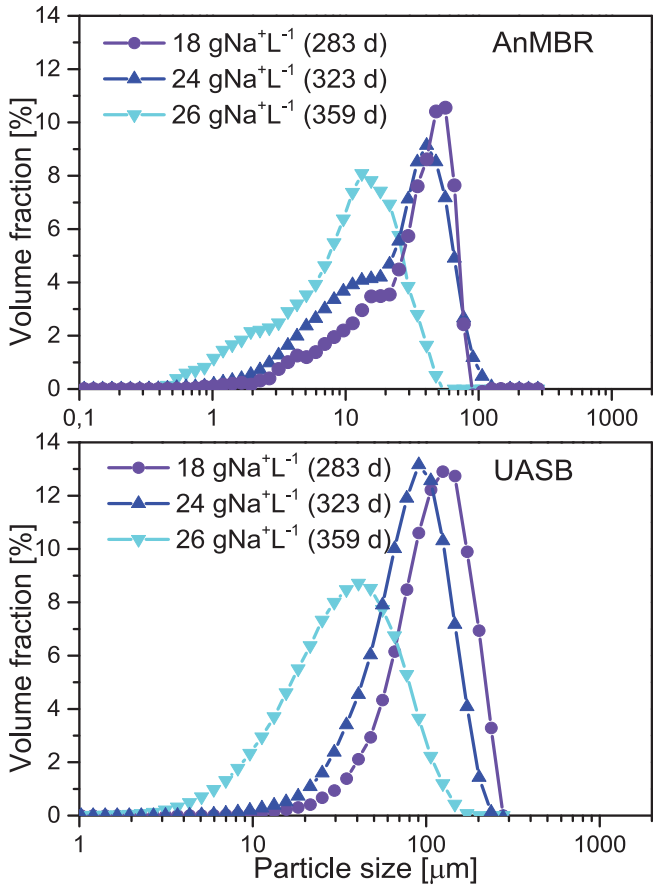

Fig. 3. Particle size distribution of biomass from AnMBR and UASB under increasing sodium concentrations.

such a condition, the addition of osmoprotectants might promote recovery of methanogenic activity [25]. In phase IV on day 379, the SMA in the UASB was 0.16 gCOD-CH_4·gVSS^{-1}·d^{-1} before the effluent phenol concentration increased in the UASB and deflocculating phenomenon occurred. It is also important to note that the rate-limiting step in phenol degradation to methane is the conversion to benzoate. The impact of high sodium and phenol concentrations could also have affected the phenol conversion step to benzoate, causing phenol accumulation in the reactor and subsequent failure of the methanogenesis [14]. The transmembrane pressure (TMP) and membrane resistance to filtration of the AnMBR indicated a stable filtration performance during the long-term operation with values of about 145 mbar and 6.8 × 10^{12} m^{-1}, respectively.

3.2. Impact of high salinity on biomass characteristics

3.2.1. Particle size distribution (PSD)

The PSD of the biomass from both reactors expressed as volume fraction % is shown in Fig. 3. After 283 days of operation and at 18 gNa$^+$·L^{-1} the biomass particle size of the UASB decreased with 57% compared to the inoculum. Thus, the UASB biomass presented a median particle size median size (D50) of about 146 μm, while the AnMBR D50 was about 56 μm. At 24 gNa$^+$·L^{-1} a greater reduction of 38% in particle size was observed in the UASB than in the AnMBR (27%). At 26 gNa$^+$·L^{-1} the particle size decreased further. The observed D50 was about 41 μm in the UASB reactor and 16 μm in the AnMBR on day 372. Previous studies have also indicated the reduction of biomass particle size under increasing salinity [16,26]. As a consequence, the UASB biomass started to wash-out, and the sludge bed collapsed at about 26 μm on day 384 as will be discussed in Section 3.2.3. The effect of

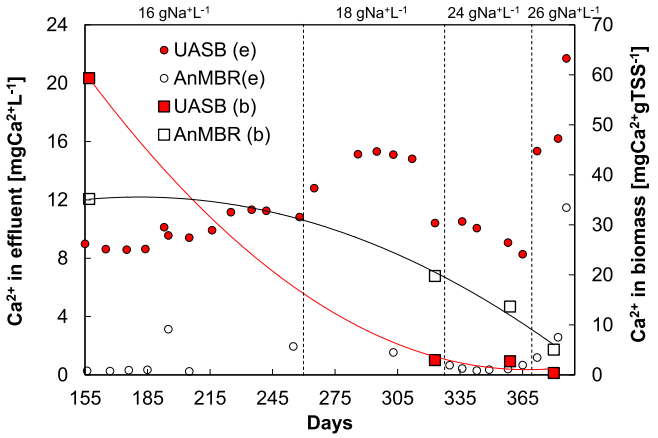

Fig. 4. Calcium concentration in the effluent (e) (left y-axis) and content in the biomass matrix (b) (right y-axis) from AnMBR and UASB reactors.

long-term calcium leaching on particle size due to high sodium concentration exposure as pictured in Fig. 4 became apparent with the noticeable particle size reduction in both reactors.

3.2.2. Extracellular polymeric substances (EPS) and soluble microbial products (SMP)

Proteins (PN) and polysaccharides (PS) were characterized as main constituents from the EPS and SMP in the biomass from both reactors at the end of each phase (Table 4). The EPS concentration was 94% PN with a content of about 66.1 ± 2.2 mg·gVSS^{-1} at 16 gNa$^+$L^{-1} in the AnMBR and about 30.2 mg·gVSS^{-1} in the UASB. A significant increase was observed from 72.9 ± 0.0 mg·gVSS^{-1} at 18 gNa$^+$L^{-1} to 107.9 ± 3.1 mg·gVSS^{-1} at 24 gNa$^+$L^{-1} in the AnMBR, whereas the EPS-PN in the UASB increased from 13.3 mg·gVSS^{-1} to 62.9 ± 0.1 mg·gVSS^{-1} at 24 gNa$^+$L^{-1}. In the case of EPS-PS, a similar increasing trend was observed in the AnMBR with the highest value at 26 gNa$^+$L^{-1}. In contrast, in the UASB the EPS-PS concentration was found to be less variable than in the AnMBR. These results do not agree with Ismail et al. [16] who observed no differences on EPS content at 10 and 20 gNa$^+$·L^{-1}, most likely because of the different feed used that contained acetate, gelatine, and starch. In fact, EPS plays an important role in self-flocculating bacteria, which has been recently presented by Huang et al. [27] as a strategy to improve saline wastewater treatment. Furthermore, the FT-IR fingerprint spectra of the EPS extracted presented in Fig. S1 showed a broad region of adsorption between 3500 and 3000 cm^{-1}, which is attributed to the O—H bond and the aromatic C—H bond in phenol [28]. A clear peak around 3450 cm^{-1} is attributed to the O—H stretching from polysaccharides [29]. The two peaks at 1634 cm^{-1} and 1440 cm^{-1} are due to N—H, C-N and C=O vibration and stretching from secondary protein structures [32]. The latter peak increased its intensity notably for the UASB at 24 gNa$^+$·L^{-1}. Additionally, the SMP PN:PS ratio was overall higher in the UASB compared to the AnMBR, with the highest value observed after the increase from 18 to 24 gNa$^+$·L^{-1} was applied, indicating a high amount of proteins solubilization. Biomass lysis products caused by the impact of an increase of 6 gNa$^+$·L^{-1} of sodium concentration might have been the reason for the higher amount of PN compared to PS. Higher production of SMP compared to EPS was observed in the UASB at a salinity exceeding 20 gNa$^+$·L^{-1} in line to what was found by Corsino et al. [30].

3.2.3. Deflocculation phenomenon: Biomass calcium leaching

Calcium washed out from the UASB biomass down to 2.7 mgCa^{2+}·gTSS^{-1} and to 0.4 mgCa^{2+}·gTSS^{-1} at 24 and 26 gNa$^+$·L^{-1}, respectively, compared to 59.3 mgCa^{2+}·gTSS^{-1} at 16 gNa$^+$·L^{-1} (Fig. 4). Apparently, calcium was leached with the high sodium concentration exposure between days 155 and 386, but increased at

Table 4
EPS and SMP in the reactors at different sodium concentrations. PN: Proteins. PS: Polysaccharides.

Sodium [$gNa^{+}\cdot L^{-1}$]	Reactor	EPS-PN [$mg\cdot gVSS^{-1}$]	EPS-PS [$mg\cdot gVSS^{-1}$]	EPS PN:PS ratio	SMP-PN [$mg\cdot gVSS^{-1}$]	SMP-PS [$mg\cdot gVSS^{-1}$]	SMP PN:PS Ratio
16	AnMBR	66.1 ± 2.2	3.5 ± 0.1	19	6.4 ± 0.0	2.2 ± 1.1	8.7
	UASB	30.2 ± 2.7	1.7 ± 0.1	18	9.0 ± 0.0	1.1 ± 0.1	8
18	AnMBR	72.9 ± 0.0	6.4 ± 0.9	11	27.8 ± 2.3	1.2 ± 0.2	22
	UASB	13.3 ± 0.7	0.8 ± 0.2	17	54.7 ± 1.5	0.8 ± 0.4	68
24	AnMBR	107.9 ± 3.1	3.5 ± 0.1	30	88.4 ± 64.3	2.5 ± 0.0	36
	UASB	62.9 ± 0.1	3.8 ± 0.0	17	87.3 ± 66.4	0.2 ± 0.2	386
26	AnMBR	104.3 ± 5.3	10.7 ± 0.4	10	61.7 ± 26.5	3.4 ± 0.5	18
	UASB	42.5 ± 0.0	3.0 ± 0.3	14	53.0 ± 9.2	2.6 ± 0.8	20

26 $gNa^{+}\cdot L^{-1}$. Concomitantly, the effluent calcium concentration increased from 9.0 $mgCa^{2+}\cdot L^{-1}$ at 16 $gNa^{+}\cdot L^{-1}$ to 15.3 $mgCa^{2+}\cdot L^{-1}$ at 18 $gNa^{+}\cdot L^{-1}$ in a period of 140 days. At 26 $gNa^{+}\cdot L^{-1}$ the UASB effluent calcium concentration increased from 15.3 $mgCa^{2+}\cdot L^{-1}$ to a maximum of 21.7 $mgCa^{2+}\cdot L^{-1}$. The permeate calcium concentration remained in a range between 0.3 and 3.1 $mgCa^{2+}\cdot L^{-1}$ in the AnMBR. At high salinity, the concentration increased from 0.4 $mgCa^{2+}\cdot L^{-1}$ at 24 $gNa^{+}\cdot L^{-1}$ to 11.5 $mgCa^{2+}\cdot L^{-1}$ at 26 $gNa^{+}\cdot L^{-1}$, indicating also a severe calcium washed out at this level of sodium concentration. Previous findings were reported by Ismail et al. [16] who observed a five-times increase in calcium concentration in the bulk liquid with an exposure of only 30 days at 20 $gNa^{+}L^{-1}$, concomitant with a reduction from 84 to 52 $mgCa^{2+}\cdot g\ TSS^{-1}$ in the biomass matrix.

Correspondingly, severe UASB biomass deflocculation was observed (Fig. 5A and C). UASB median particle size decreased from 117 ± 82 μm at 24 $gNa^{+}\cdot L^{-1}$ to 26 ± 22 μm at 26 $gNa^{+}\cdot L^{-1}$ (Fig. 5B and D), indicating a clear disruption of the sludge bed due to high salinity. This supports the hypothesis that high sodium concentration reduces sludge strength by replacing calcium from the biomass matrix, thereby producing a weak dispersed sludge [10].

In our study, the conductivity was also measured and values over a range from 43 $mS\cdot cm^{-1}$ to 58 $mS\cdot cm^{-1}$ were observed. De Vrieze et al. [26] suggested that with high salinity an increase in conductivity up to 45 $mS\cdot cm^{-1}$ caused granular sludge disintegration and biomass washout. A substantial reduction in particle size from about 1290 to 54 μm was also associated with exposure to high salinity. In contrast to the observed deflocculation in our study, Li et al. [8] observed that granule size increased with higher sodium concentrations in a UASB up to 11.2 $gNa^{+}\cdot L^{-1}$ treating saline sulfate wastewater. Similarly, Sudmalis et al. [31] managed to obtain larger granules at 20 $gNa^{+}\cdot L^{-1}$ than

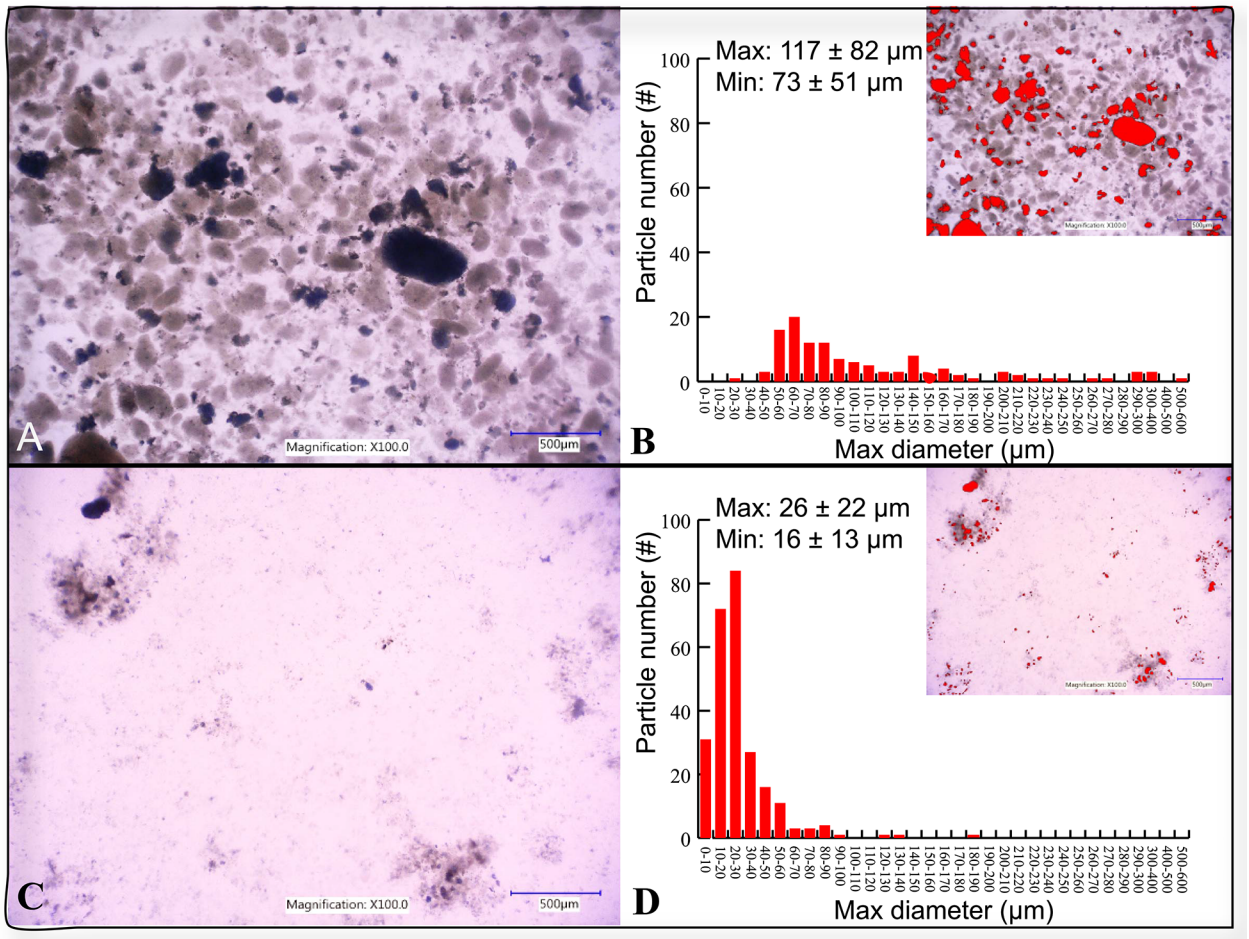

Fig. 5. Deflocculation phenomenon. A. Observation of biomass under microscope before UASB deflocculated. B. Particle size before UASB deflocculated. C. Observation of biomass under microscope after UASB deflocculated. D. Particle size after UASB deflocculated.

at 5 $gNa^{+}{\cdot}L^{-1}$ with comparable granule strength, implying that in this case strength was not affected by high sodium concentrations. This UASB reactor was fed with 13 $mgCa^{2+}{\cdot}L^{-1}$ during the initial 90 days of operation from a total of 217 days. In our study, the feed contained 100 times lower calcium concentration (0.14 $mgCa^{2+}{\cdot}L^{-1}$) and a longer-term of operation was applied. Calcium leaching occurred apparently faster in the AnMBR with a reduction in the calcium content in the biomass matrix and an increase in calcium content in the permeate at high salinity, implying that calcium leaching is rather related to biomass properties rather than to reactor configuration. However, despite the fact that calcium can support granulation by forming cationic bridges with extracellular polymeric substances (EPS) [32], other studies have shown that concentrations higher than 1 $gCa^{2+}{\cdot}L^{-1}$ [33] have no positive effects on granulation and even detrimental effects on microbial activity. Kobayashi et al. [34] indicated that calcium addition (0.32–0.64 $gCa^{2+}{\cdot}L^{-1}$) accelerated biofilm formation but this positive effect is strongly counteracted by sodium concentrations as low as 3.45 $gNa^{+}{\cdot}L^{-1}$ due to competition for limited cation binding sites. The different results suggest that cationic bridges formation at high sodium concentrations for cell aggregation are still not well understood. Antagonistic or synergistic effects with other cations like potassium [15,35] also cannot be overlooked.

3.3. Microbial community comparison

3.3.1. Microbial community structure and dynamics

Microbial community analysis resulted in 48841 ± 21479 reads and 958 OTUs in the UASB, while 56951 ± 5381 reads and 944 OTUs were obtained in the AnMBR. Microbial community structure of the reactor biomass was analyzed by next-generation sequencing targeting the 16S rRNA gene along the different operational phases. At the order level (Fig. 6A), the most dominant bacteria in the reactors (UASB, AnMBR) were Clostridiales (16.66%, 15.61%), Natranaerobiales (9.83%, 6.89%), Synergistales (3.78%, 3.95%), BA021 (3.52%, 5.42%), Thermotogales (1.25%, 5.36%) and Bacteroidales (8.21%) in the UASB. Methanosarcinales (46.86%) was the dominant Archaea in the UASB and Methanobacteriales (26.22%) and Methanosarcinales (23.99%) in the AnMBR.

Further in phase I, at 0.11 PhLR and after longer exposure to 16 $gNa^{+}L^{-1}$, the Methanosarcinales and Natranaerobiales increased to 53.76% and 11.84% in the UASB, and to 37.34%, and 8.50% in the AnMBR, respectively. The decrease in relative abundance was observed mainly in Bacteroidales (5.22%), BA021 (1.18%) and Synergistales (2.71%) in the UASB, whereas in the AnMBR BA021 and Thermotogales decreased to 4.42% and 3.63%, respectively. In phase II, at 18 $gNa^{+}{\cdot}L^{-1}$, *Methanosaeta*, belonging to Methanosarcinales order increased from 47.04% to 59.30% as the PhLR increased from 0.33 to 1.11 $gPh{\cdot}L^{-1}{\cdot}d^{-1}$ in the UASB, while in the case of the AnMBR both the *Methanobacterium* and *Methanosaeta* decreased from 9.23%, and 45.72% to 8.33% and 35.63%, respectively (Fig. 6B). *Marinobacter* (5.35%), *Halomonas* (8.12%) and *Marinobacterium* (2.81%) all belonging to Gammaproteobacteria class (see Fig. S2) and involved in aromatics degradation, together with the genus *Paracoccus* (6.86%, Alphaproteobacteria), increased significantly in the UASB at 0.33 $gPh{\cdot}L^{-1}{\cdot}d^{-1}$ on day 280 in phase II. In contrast, all previous Proteobacteria were present in the AnMBR with a relative abundance lower than 0.5%. However, at a higher PhLR and higher salinity in further phases, all Proteobacteria decreased more than five-fold their relative abundance in the UASB most likely due to sensitivity to high sodium. Wang et al. [14] related a decrease in relative abundance of Proteobacteria with a reduction in phenol conversion under high salinity. The AnMBR exhibited an increase in the Bacteroidales (ML635J-40), and the genus *Clostridium* and *Pelotomaculum* of about 22%, 25% and 17% due to the increase in PhLR, indicating their involvement in the phenol degradation. Proteobacteria, Firmicutes (*Clostridium*, Natranaerobiales, *Pelotomaculum*), and Bacteroidetes (Bacteroidales) have been reported as the main phyla in anaerobic reactors treating phenolic wastewater [14,36].

In phase III, at 24 $gNa^{+}L^{-1}$ and 0.67 $gPh{\cdot}L^{-1}{\cdot}d^{-1}$, *Methanobacterium* (16.14%), *Methanosaeta* (39.33%), *Clostridium*

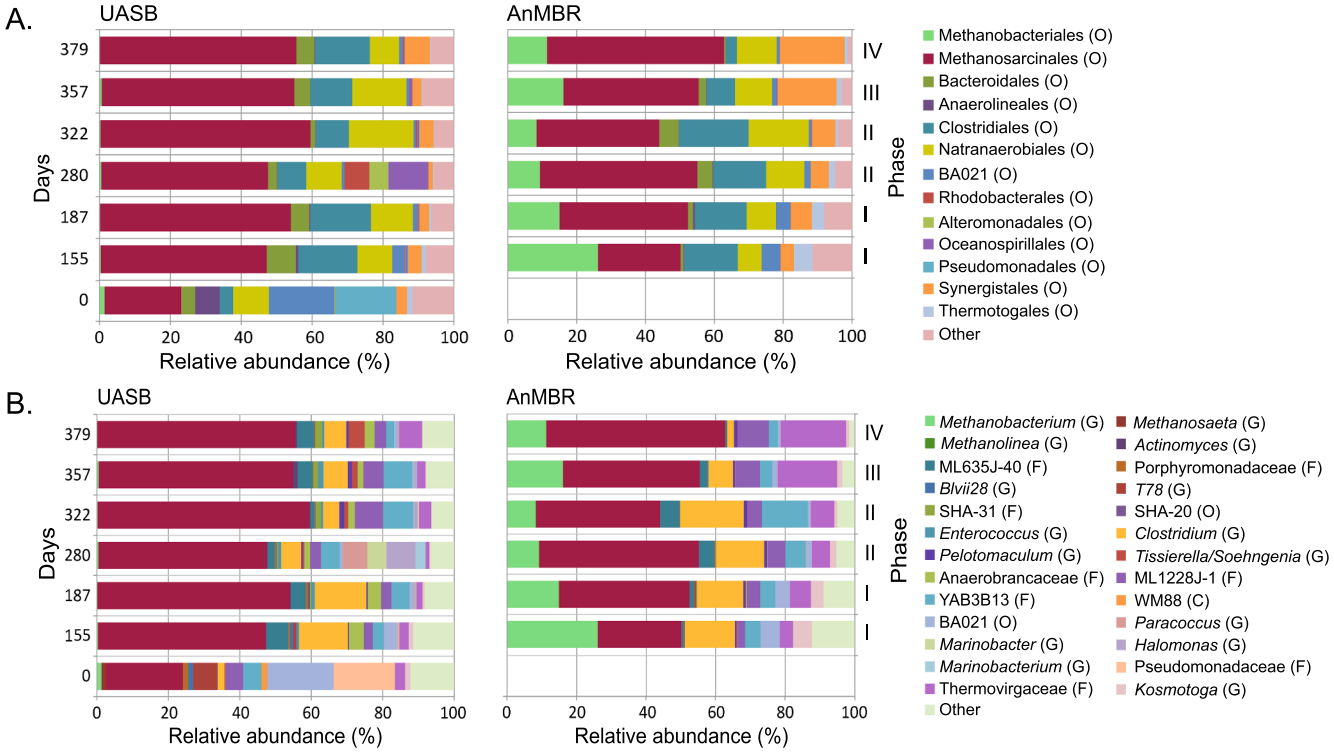

Fig. 6. Microbial community composition of the UASB and AnMBR treating phenolic wastewater at increasing salinity. A. Order level B. up to Genus level. Relative abundance cutoff at 1%.

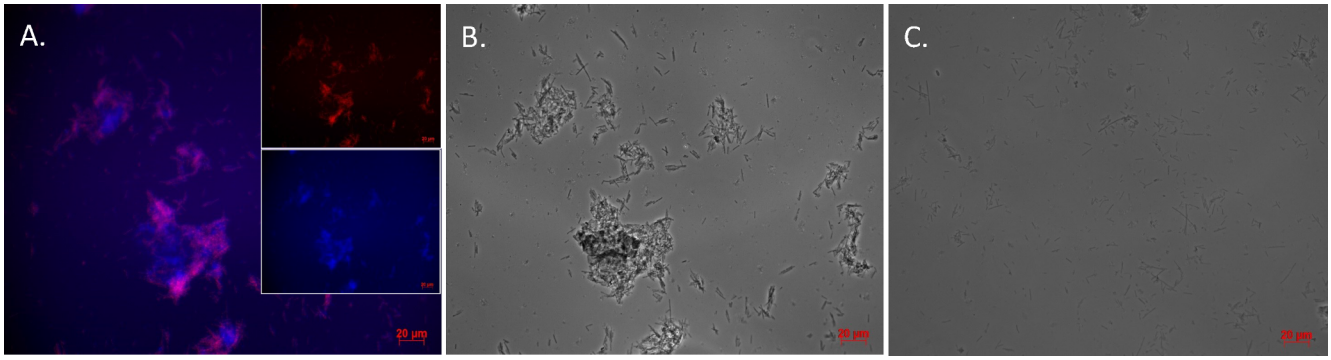

Fig. 7. A. FISH from UASB reactor. B. Sludge morphology in UASB , C. Sludge morphology in AnMBR after 371 days of operation. The samples were hybridized with the probe specific for archaea (ARC915, red) and were stained with DAPI (blue). Scale bar = 20 µm.

(7.01%), Natranaerobiales (7.10% ML1228J-1; 3.56% YAB3B13) and Synergistales (17.06%, Thermovirgaceae) dominated in the AnMBR. This could potentially suggest a shift induced by high salinity from acetoclastic methanogenesis to syntrophic acetate oxidation coupled with hydrogenotrophic methanogenesis, as reported earlier for Clostridiales [37]. Thermovirgaceae increased about two-fold within phase I and III when the highest soluble protein (SMP-PN) content was observed in the AnMBR corresponding with its protein/amino acid degradation nature. Conversely, the UASB presented a higher variability than the AnMBR in the bacterial relative abundance. SBR1031 (1.31%, SHA-31), *Enterococcus* (1.51%), *Clostridium* (6.77%), *Pelotomaculum* (1.16%), *Tissierella Soehngenia* (1.60%), Natranaerobiales (1.57%, Anaerobrancaceae; 5.69%, ML1228J-1; 7.98%, YAB3B13) and Synergistales (2.27%, Thermovirgaceae) were the most abundant microorganisms. *Methanosaeta* (54.35%) dominated as Archaea (Fig. 6B). FISH (Fig. 7A) confirmed the dominance of archaeal filamentous cells in the UASB, positive to the ARC915 probe (in red) after 371 days of operation. There was a clear difference in the morphology of the biomass cells. In the UASB robust and long filaments in conglomerates were observed (Fig. 7B). In the AnMBR (Fig. 7C) the cells mainly had a single filament morphology without the presence of clusters.

In phase IV, at 26 $gNa^+ \cdot L^{-1}$and the same PhLR as in phase III, *Methanosaeta* remarkably increased to 51.46% in the AnMBR, while *Methanobacterium* decreased its relative abundance to 11.37%. High sodium concentrations apparently resulted in a strong increase in abundance of *Methanosaeta*, which was not the case for the other methanogens, confirming that at high salinity, salt-tolerant methane-producing archaea can be enriched [38]. However, as also observed by De Vrieze et al. [22], this high abundance does not automatically reflect a high activity, which could explain the lower SMA at 24 and 26 $gNa^+ \cdot L^{-1}$. Only in the AnMBR, hydrogenotrophic methanogens were present in relatively high abundance. *Pelotomaculum,* a syntrophic aromatic compound degrader, presented the highest abundance in this phase whereas Clostridiales decreased to 3.2% (Fig. 6A). In the UASB, an increase of 3.70% in relative abundance from Clostridiales, 4.56% of Synergistales (Thermovirgaceae), and the decrease of Natranaerobiales from 15.31% to 8.27% were observed.

The changes in community structure over time, and with respect to the different salinity and phenol loading rates applied was analyzed by non-metric distance scaling (NMDS) (Fig. S3). The NMDS analysis indicated that the microbial community in the AnMBR and UASB reactor shifted due to the increase in salinity conditions and phenol loading rate and were dissimilar even though they were exposed to similar operational conditions. Three distinct clusters could be identified, containing the inoculum, UASB and AnMBR reactors samples. The analysis of similarity (ANOSIM) statistical test demonstrated significant differences ($p = 0.04$) of the microbial community composition and a high separation ($R = 0.68$) for both reactors. Furthermore, ADONIS statistical test revealed that in the UASB the microbial composition at 16$gNa^+ \cdot L^{-1}$ was significantly different ($p = 0.01$, $R^2 = 0.42$) compared to the samples exposed to higher salinity, whereas in the AnMBR the microbial population at 26 $gNa^+ \cdot L^{-1}$ showed significant differences ($p = 0.01$, $R^2 = 0.32$), compared to the phases under lower sodium concentrations.

3.3.2. Microbial community diversity analysis

The change in microbial community structure in response to a disturbance such as an increase in salinity was evaluated via alpha diversity analysis using the Hill diversity order numbers approach [20]. Differences were observed among the three Hill diversity orders for the microbial community of the UASB and AnMBR. A higher richness (H_0) was observed in the UASB compared to the AnMBR in Phase I and Phase IV (Fig. 8A), while this was not the case for Phases II and III.

The diversity in AnMBR (H_1), i.e., the abundance of all species and evenness ratio, was comparable to the UASB under the applied conditions (Fig. 8B) without significant differences along the phases ($p = 0.11$).

The H_2 diversity in the AnMBR was higher than for the UASB in phase I (57%), phase II (48%) and phase III (36%), demonstrating that there were more dominant species in the AnMBR (Fig. 8C). High species richness and diversity are related to increased resilience, as a larger pool of microorganisms augments the probability to maintain functionality to respond to disturbances such high salinity [39]. Furthermore, the species evenness (Fig. 8D) of the AnMBR was significantly higher than that of the UASB in all phases ($p = 0.047$), representing a more stable community composition. This is in line with the observation that microbial communities with greater evenness exhibit higher methanogenic robustness. A more even community has a higher potential to use redundant functional pathways under perturbations, leading to a more stable anaerobic digestion process [40].

Overall, the AnMBR exhibited better stability and more efficient treatment under long-term high sodium concentrations than the UASB. The question that remains under discussion is whether under random sodium concentration fluctuations a membrane enhanced retention system can permanently maintain microbial stability and robust performance. Further research could, for example, evaluate whether an online calcium supply control strategy can minimize the impact of high sodium concentration on biomass properties when calcium leaching takes place independently of the reactor configuration. The findings of this study highlight the potentials for the AnMBR technology application for chemical wastewater streams under extreme conditions that are more difficult to be overcome by conventional high rate anaerobic technologies such as a UASB.

4. Conclusions

This study focused on the comparative assessment of a UASB reactor and an AnMBR with respect to the phenol degradation under high

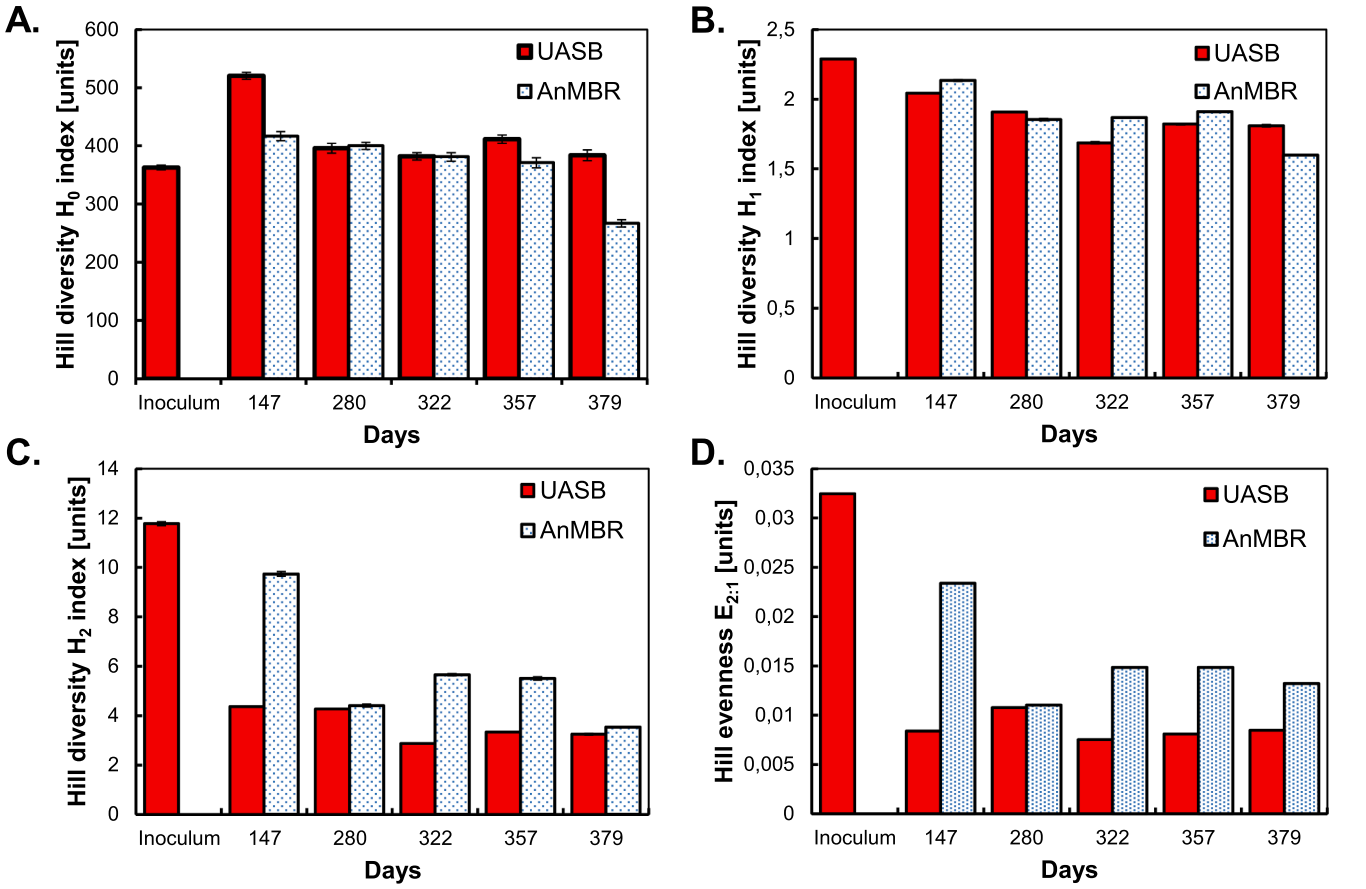

Fig. 8. Alpha diversity of UASB and AnMBR. A. H_0 (richness, number of OTUs). B. H_1 (exponential value of the Shannon index). C. H_2 (inverse Simpson index). D. $E_{2:1}$ (species evenness) were calculated both for bacteria and archaea.

salinity conditions. The AnMBR process exhibited better stability and performance than the UASB for the treatment of the phenolic wastewater over a range of 16–26 $gNa^{+}{\cdot}L^{-1}$. Under highest sodium concentration the UASB phenol conversion rate decreased from 103.2 to 32.9 $mgPh.gVSS^{-1}{\cdot}d^{-1}$, and a COD removal of 47% was observed before biomass washout occurred. The AnMBR exhibited a phenol and COD removal of 96% and 80%, respectively, demonstrating that a membrane enhanced biomass retention was able to overcome the impact of high salinity. An increase of 6 $gNa^{+}{\cdot}L^{-1}$ produced high solubilization of protein-like substances in both reactors and a decrease in median particle size of 38% and 27% in the UASB and AnMBR, respectively. Moreover, at 26 $gNa^{+}{\cdot}L^{-1}$ and phenol concentration of 3 $gPh.L^{-1}$, the UASB biomass deflocculated due to a long-term calcium wash-out from 59.3 $mgCa^{+}{\cdot}gTSS^{-1}$ at 16 $gNa^{+}{\cdot}L^{-1}$ to 0.4 $mgCa^{2+}{\cdot}gTSS^{-1}$, leading to reactor failure. Concomitantly, a median particle size reduction in both reactors to about 26 µm in the UASB and 16 µm in the AnMBR revealed a clear impact of the increase in sodium concentration on biomass aggregation. Additionally, high salinity promoted a higher variability in microbial community composition on the genus level in the UASB compared to the AnMBR, which reflects the susceptibility of certain microorganisms in biofilms to high salinity. Hence, the AnMBR showed significantly higher species evenness than the UASB, exhibiting higher methanogenic activity due to its greater probability to maintain functionality and to respond to disturbances such as high phenol and sodium concentration increases.

Overall, this study demonstrated that two high-rate anaerobic reactor configurations with different biomass retention systems (biofilm-granule in UASB and membrane in AnMBR) resulted in a diverse performance and stability when treating phenolic wastewater under high salinity.

Acknowledgments

This research is supported by the Dutch Technology Foundation (STW, Project No.13348), which is part of the Netherlands Organization for Scientific Research (NWO), partly funded by the Dutch Ministry of Economic Affairs. This research is co-sponsored by Evides Industriewater and Paques B.V. The authors thank Dr. Revanuru Subramanyan for his contribution with the start-up phase of the UASB reactor.

Appendix A. Supplementary data

Supplementary data to this article can be found online at https://doi.org/10.1016/j.cej.2019.02.097.

References

[1] A. Yurtsever, B. Calimlioglu, M. Görür, Ö. Çınar, E. Sahinkaya, Effect of NaCl concentration on the performance of sequential anaerobic and aerobic membrane bioreactors treating textile wastewater, Chem. Eng. J. 287 (2016) 456–465.
[2] F. Rosenkranz, L. Cabrol, M. Carballa, A. Donoso-Bravo, L. Cruz, G. Ruiz-Filippi, R. Chamy, J.M. Lema, Relationship between phenol degradation efficiency and microbial community structure in an anaerobic SBR, Water Res. 47 (2013) 6739–6749.
[3] Y. Jiang, L. Wei, H. Zhang, K. Yang, H. Wang, Removal performance and microbial communities in a sequencing batch reactor treating hypersaline phenol-laden wastewater, Bioresour. Technol. 218 (2016) 146–152.
[4] X. Su, Y. Wang, B. Xue, M.Z. Hashmi, H. Lin, J. Chen, Z. Wang, R. Mei, F. Sun, Impact of resuscitation promoting factor (Rpf) in membrane bioreactor treating high-saline phenolic wastewater: performance robustness and Rpf-responsive bacterial populations, Chem. Eng. J. 357 (2019) 715–723.
[5] W. Wang, K. Yang, J. Muñoz Sierra, X. Zhang, S. Yuan, Z. Hu, Potential impact of methyl isobutyl ketone (MIBK) on phenols degradation in an UASB reactor and its degradation properties, J. Hazard. Mater. 333 (2017) 73–79.

[6] J.D. Muñoz Sierra, W. Wang, D. Cerqueda-Garcia, M.J. Oosterkamp, H. Spanjers, J.B. van Lier, Temperature susceptibility of a mesophilic anaerobic membrane bioreactor treating saline phenol-containing wastewater, Chemosphere 213 (2018) 92–102.
[7] J.B. van Lier, F.P. van der Zee, C.T.M.J. Frijters, M.E. Ersahin, Celebrating 40 years anaerobic sludge bed reactors for industrial wastewater treatment, Rev. Environ. Sci. Biotechnol. 14 (2015) 681–702.
[8] J. Li, L. Yu, D. Yu, D. Wang, P. Zhang, Z. Ji, Performance and granulation in an upflow anaerobic sludge blanket (UASB) reactor treating saline sulfate wastewater, Biodegradation 25 (2014) 127–136.
[9] J. Yang, H. Spanjers, D. Jeison, J.B. Van Lier, Impact of Na+ on biological wastewater treatment and the potential of anaerobic membrane bioreactors: a review, Critical Rev. Environ. Sci. Technol. 43 (2013) 2722–2746.
[10] D. Jeison, A. Del Rio, J.B. Van Lier, Impact of high saline wastewaters on anaerobic granular sludge functionalities, Water Sci. Technol. 57 (2008) 815–819.
[11] R.K. Dereli, M.E. Ersahin, H. Ozgun, I. Ozturk, D. Jeison, F. van der Zee, J.B. van Lier, Potentials of anaerobic membrane bioreactors to overcome treatment limitations induced by industrial wastewaters, Bioresour. Technol. 122 (2012) 160–170.
[12] D.C. Stuckey, Recent developments in anaerobic membrane reactors, Bioresour. Technol. 122 (2012) 137–148.
[13] J.D. Muñoz Sierra, C. Lafita, C. Gabaldón, H. Spanjers, J.B. van Lier, Trace metals supplementation in anaerobic membrane bioreactors treating highly saline phenolic wastewater, Bioresour. Technol. 234 (2017) 106–114.
[14] W. Wang, B. Wu, S. Pan, K. Yang, Z. Hu, S. Yuan, Performance robustness of the UASB reactors treating saline phenolic wastewater and analysis of microbial community structure, J. Hazard. Mater. 331 (2017) 21–27.
[15] J.D. Muñoz Sierra, M.J. Oosterkamp, W. Wang, H. Spanjers, J.B. van Lier, Impact of long-term salinity exposure in anaerobic membrane bioreactors treating phenolic wastewater: performance robustness and endured microbial community, Water Res. 141 (2018) 172–184.
[16] S.B. Ismail, C.J. de La Parra, H. Temmink, J.B. van Lier, Extracellular polymeric substances (EPS) in upflow anaerobic sludge blanket (UASB) reactors operated under high salinity conditions, Water Res. 44 (2010) 1909–1917.
[17] M.C.v. Loosdrecht, P.H. Nielsen, C.M. Lopez-Vazquez, D. Brdjanovic, Experimental methods in wastewater treatment, Water Intell (2016).
[18] R. Edgar UCHIME2: improved chimera prediction for amplicon sequencing, bioRxiv, 2016.
[19] R.C. Edgar, Search and clustering orders of magnitude faster than BLAST, Bioinformatics 26 (2010) 2460–2461.
[20] M.O. Hill, Diversity and evenness: a unifying notation and its consequences, Ecology 54 (1973) 427–432.
[21] M.K.H. Winkler, J.P. Bassin, R. Kleerebezem, L.M.M. de Bruin, T.P.H. van den Brand, M.C.M. van Loosdrecht, Selective sludge removal in a segregated aerobic granular biomass system as a strategy to control PAO–GAO competition at high temperatures, Water Res. 45 (2011) 3291–3299.
[22] J. De Vrieze, L. Regueiro, R. Props, R. Vilchez-Vargas, R. Jáuregui, D.H. Pieper, J.M. Lema, M. Carballa, Presence does not imply activity: DNA and RNA patterns differ in response to salt perturbation in anaerobic digestion, Biotechnol. Biofuels 9 (2016) 244.
[23] S. Aslan, N. Şekerdağ, Salt inhibition on anaerobic treatment of high salinity wastewater by upflow anaerobic sludge blanket (UASB) reactor, Desalination Water Treatment 57 (2016) 12998–13004.
[24] O. Chapleur, C. Madigou, R. Civade, Y. Rodolphe, L. Mazéas, T. Bouchez, Increasing concentrations of phenol progressively affect anaerobic digestion of cellulose and associated microbial communities, Biodegradation 27 (2016) 15–27.
[25] L. Zhang, K. Zhu, A. Li, Differentiated effects of osmoprotectants on anaerobic syntrophic microbial populations at saline conditions and its engineering aspects, Chem. Eng. J. 288 (2016) 116–125.
[26] J. De Vrieze, M. Coma, M. Debeuckelaere, P. Van der Meeren, K. Rabaey, High salinity in molasses wastewaters shifts anaerobic digestion to carboxylate production, Water Res. 98 (2016) 293–301.
[27] Z. Huang, Y. Wang, L. Jiang, B. Xu, Y. Wang, H. Zhao, W. Zhou, Mechanism and performance of a self-flocculating marine bacterium in saline wastewater treatment, Chem. Eng. J. 334 (2018) 732–740.
[28] Z. Wang, Z. Wu, S. Tang, Extracellular polymeric substances (EPS) properties and their effects on membrane fouling in a submerged membrane bioreactor, Water Res. 43 (2009) 2504–2512.
[29] R.K. Dereli, B. Heffernan, A. Grelot, F.P. van der Zee, J.B. van Lier, Influence of high lipid containing wastewater on filtration performance and fouling in AnMBRs operated at different solids retention times, Separation Purif. Technol. 139 (2015) 43–52.
[30] S.F. Corsino, M. Capodici, M. Torregrossa, G. Viviani, Physical properties and extracellular polymeric substances pattern of aerobic granular sludge treating hypersaline wastewater, Bioresour. Technol. 229 (2017) 152–159.
[31] D. Sudmalis, M.C. Gagliano, R. Pei, K. Grolle, C.M. Plugge, H.H.M. Rijnaarts, G. Zeeman, H. Temmink, Fast anaerobic sludge granulation at elevated salinity, Water Res. 128 (2018) 293–303.
[32] Y. Shi, J. Huang, G. Zeng, Y. Gu, Y. Chen, Y. Hu, B. Tang, J. Zhou, Y. Yang, L. Shi, Exploiting extracellular polymeric substances (EPS) controlling strategies for performance enhancement of biological wastewater treatments: an overview, Chemosphere 180 (2017) 396–411.
[33] M.C. Gagliano, S.B. Ismail, A.J.M. Stams, C.M. Plugge, H. Temmink, J.B. Van Lier, Biofilm formation and granule properties in anaerobic digestion at high salinity, Water Res. 121 (2017) 61–71.
[34] T. Kobayashi, Y. Hu, K.-Q. Xu, Impact of cationic substances on biofilm formation from sieved fine particles of anaerobic granular sludge at high salinity, Bioresour. Technol. 257 (2018) 69–75.
[35] T. Onodera, K. Syutsubo, M. Hatamoto, N. Nakahara, T. Yamaguchi, Evaluation of cation inhibition and adaptation based on microbial activity and community structure in anaerobic wastewater treatment under elevated saline concentration, Chem. Eng. J. 325 (2017) 442–448.
[36] C. Madigou, S. Poirier, C. Bureau, O. Chapleur, Acclimation strategy to increase phenol tolerance of an anaerobic microbiota, Bioresour. Technol. 216 (2016) 77–86.
[37] B. Müller, L. Sun, M. Westerholm, A. Schnürer, Bacterial community composition and FHS profiles of low- and high-ammonia biogas digesters reveal novel syntrophic acetate-oxidising bacteria, Biotechnol. Biofuels 9 (2016) 48.
[38] Y. Wu, X. Wang, M.Q.X. Tay, S. Oh, L. Yang, C. Tang, B. Cao, Metagenomic insights into the influence of salinity and cytostatic drugs on the composition and functional genes of microbial community in forward osmosis anaerobic membrane bioreactors, Chem. Eng. J. 326 (2017) 462–469.
[39] J.J. Werner, D. Knights, M.L. Garcia, N.B. Scalfone, S. Smith, K. Yarasheski, T.A. Cummings, A.R. Beers, R. Knight, L.T. Angenent, Bacterial community structures are unique and resilient in full-scale bioenergy systems, Proc. Natl. Acad. Sci. 108 (2011) 4158–4163.
[40] L. Wittebolle, M. Marzorati, L. Clement, A. Balloi, D. Daffonchio, K. Heylen, P. De Vos, W. Verstraete, N. Boon, Initial community evenness favours functionality under selective stress, Nature 458 (2009) 623.